Proceedings of the 5th International Workshop on New Photon-Detectors (PD18)
Downloaded from journals.jps.jp by Deutsches Elek Synchrotron on 12/12/19

Proc. 5th Int. Workshop New Photon-Detectors (PD18)
JPS Conf. Proc. **27**, 011002 (2019)
https://doi.org/10.7566/JPSCP.27.011002

High-Density Silicon Photomultipliers with Epitaxial Quenching Resistors at Novel Device Laboratory

Hongmin Liu[1], Kun Liang[1,2*], Baicheng Li[1], Yu Pen[1], Lei Dai[1], Ru Yang[1,2] and Dejun Han[1,2]

[1]*Novel Device Laboratory, College of Nuclear Science and Technology, Beijing Normal University, 100875, Beijing, China*
[2]*Beijing Radiation Center, Beijing, China*

**E-mail: lk@bnu.edu.cn*
(Received February 27, 2019)

Abstract：Silicon photomultiplier with epitaxial quenching resistor (EQR SiPM) uses the bulk resistors of the epitaxial layer as the quenching resistors, it features high microcell density, high photon detection efficiency (PDE) and fast response to even a single photon. This report details the latest progress of EQR SiPM at Novel Device Laboratory (NDL). The PDE was precisely characterized by using both improved photon counting method and Poisson statistics method. Typically, the EQR SiPMs, with P-on-N diode configuration and 10000 individual cells within 1×1 mm^2 active area, demonstrated a dark count rate of 700 kHz at 7 V overvoltage, peak PDE of ~34% at 420 nm, single-photon time resolution (SPTR) of 53 ps (FWHM) and the recovery time of 2.2 ns. Those performances show that the EQR SiPM is very suitable to be applied in a calorimeter of high energy physics where large dynamic range and high PDE are needed simulaneously.

KEYWORDS: Silicon Photomultiplier (SiPM), Epitaxial Quenching Resistor (EQR), Photon Detection Efficiency (PDE)

1. Introduction

Silicon photomultipliers (SiPMs) are finding more and more applications in high energy physics, astrophysics, nuclear medical imaging, fluorescence spectroscopy and other low level light detections due to their advantages such as high gain, low bias voltage, excellent timing properties, robustness and insensitivity to magnetic fields [1]. Most commercial SiPM products, including those manufactured by SensL, Hamamatsu etc., employ highly resistive poly-silicon or thin metal film to make the quenching resistors for the SiPMs. Those devices have a drawback that the PDE is conflicted to the microcell density (i.e., dynamic range). For example, C-10010-SMT from SensL with 1×1 mm^2 active area and 2880 microcells has only peak PDE of 18% at 420 nm [2]. S12571-010-C/P from Hamamatsu with 1×1 mm^2 active area and 10000 microcells has only peak PDE of 10% at 470nm [3].

In the past years, Novel Device Laboratory (NDL) has been developing a SiPM technology, so called EQR SiPMs that employs the bulk silicon resistors of epitaxial layer to form the quenching resistor. As shown in Fig.1, the device consists of N-enriched regions forming high electric field between N-type epitaxial silicon wafer and P++ surface layer. The depletion regions in the gap P-N junction electrically isolate the APD microcells. The P++ channel function as a common anode to directly collect avalanche signals from each microcell, and the epitaxial region below the P-N junction functions as the quenching resistor to quench the avalanche multiplication and make the microcell recovery.

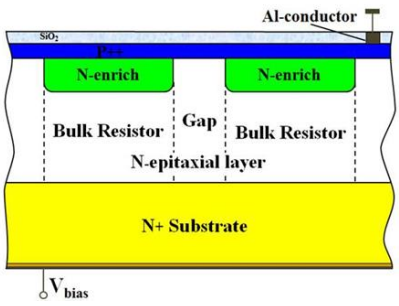

Fig.1. The schematic structure of EQR SiPM.

Owing to effectively resolving the “dead regions” formed by the poly-silicon or thin metal film quenching resistors on device surface, the aluminum strips and the guard-

©2019 The Author(s)

This article is published by the Physical Society of Japan under the terms of the Creative Commons Attribution 4.0 License. Any further distribution of this work must maintain attribution to the author(s) and the title of the article, journal citation, and DOI.

Proceedings of the 5th International Workshop on New Photon-Detectors (PD18)
Downloaded from journals.jps.jp by Deutsches Elek Synchrotron on 12/12/19

ring spaces resulting the conflict between photon detection efficiency (PDE, proportional to fill factor) and dynamic range (proportional to microcell density), the EQR SiPMs feature small microcell size (high density), high PDE while retaining large dynamic range, fast response to even a single photon [4]. Besides, no extra fabrication processes for quenching resistors are needed, thus simple and cost effective fabrication technology can be realized.

In this paper, the latest progress on EQR SiPMs with P-on-N diode configuration, active area of 1×1 mm^2 and 3×3 mm^2, microcell size of 10×10 μm^2 (density ~10000/mm^2) or 12.5×12.5 μm^2 (density ~8000/mm^2) are reported. The peak PDE of ~34% at 420 nm, single-photon time resolution (SPTR) of 53 ps (FWHM) and the recovery time of 2.2 ns for the 1×1 mm^2 EQR SiPM with microcell size of 10×10 μm^2 were characterized for their potential applications in astrophysics, high energy physics and nuclear medicine imaging.

2. Experimental Setup and Method

The EQR SiPM was firstly measured in dark conditions to accomplish the noise analysis. In a millisecond-long time window, the output signals are acquired and stored by a digital oscilloscope (LeCroy WaveRunner 640Zi) with the sampling rate of the scope as 20 Gs/s and the bandwidth as 1 GHz. Using Matlab program to analyze the amplitude and arrival time for each pulse. The total dark pulse distribution can be obtained. Due to different generation mechanism, it is easy to distinguish the delayed-correlated noise component (mainly consisting of afterpulsing and delayed crosstalk) and the primary dark noise.

In lighting circumstance, the PDE against wavelength has been characterized with photon counting method by counting the light pulses to random low light [5]. As shown in Fig.2 (a), light from Xenon lamp through a monochromator illuminated the SiPM and a monitoring PIN uniformly through a integrating sphere. The amplified photon counting pulses from SiPM were recorded by a digital oscilloscope (Tektronic TDS 1012), and the photocurrent from PIN were collected by Keithley 2635B Source Measure Unit (SMU). The PDE was calculated by the following formula:

$$PDE = \frac{(CR-DCR)*R_{PIN}*h*c}{(I_{total}-I_{dark})*\lambda} \times \frac{A_{PIN}}{A_{SiPM}} \times 100\% \quad (1)$$

Where, DCR is dark count rate and CR is photon counting rate of SiPM over 0.5 p.e. (photoelectron) threshold; h represents Planck constant, c represents vacuum light speed and λ represents wavelength; R_{PIN} is spectral responsivity, I_{total} is photocurrent and I_{dark} is dark current of PIN; A_{SiPM} and A_{PIN} are active areas of SiPM and PIN respectively.

It is noting that, high probability of the afterpulsing and the delayed crosstalk may be recorded as light pulse count, which results in overestimation for PDE. Moreover, pile-up pulses make it difficult to identify events, and cause misjudgment on PDE. In our experiment, the modified PDE results were calculated after deducting the delayed-correlated noise component from the optical response count and was proved to be reliable.

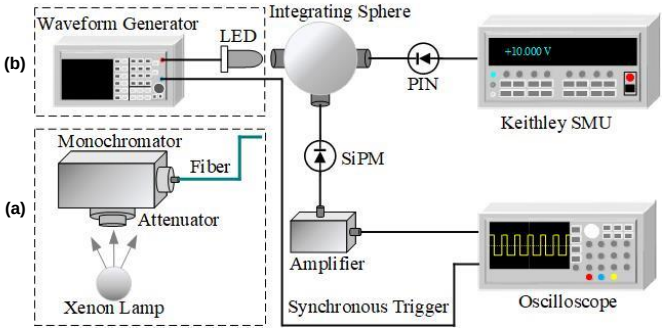

Fig.2. The experimental setup for characterizing the PDE with (a) photon counting method and (b) Poisson method.

The PDE has also been measured with Poisson method basing on statistical analysis [6]. As shown in Fig.2 (b), the pulse light from LED with frequency of 1 MHz and pulse width of 16 ns illuminated the SiPM and the PIN. The signals from SiPM were

Proceedings of the 5th International Workshop on New Photon-Detectors (PD18)
Downloaded from journals.jps.jp by Deutsches Elek Synchrotron on 12/12/19

recorded by a digital oscilloscope (LeCroy WaveRunner 640Zi) that was triggered to the waveform generator. According to the Poisson statistical principle, the average number of photoelectrons before and after illumination could be determined, hence the number of net photoelectrons was obtained. The PDE can be expressed as [5,7]:

$$PDE = \frac{(\mu_{light}-\mu_{dark})*R_{PIN}*h*f*c}{(I_{total}-I_{dark})*\lambda} \times \frac{A_{PIN}}{A_{SiPM}} \times 100\% \quad (2)$$

Where, μ_{light} is the average number of photoelectrons detected in light condition and μ_{dark} is in dark condition, f is the frequency of the light source. The Poisson method can effectively deduct noise components to get actual photon detection efficiency.

By gradually increasing the light intensity, the dynamic range can be characterized. Moreover, the dynamic range is the difference between the number of incident photons required to excite all microcells and one microcell [8,9]. Time resolution reflects the accuracy of SiPM to measure the arrival time of a single photon signal. Its measurement method is detailed at reference [10,11]. The recovery time of the microcell can be studied by analyzing waveform in dark condition and extracting afterpulsing events [12].

3. Results and Discussion

3.1 Noise Analysis

For the EQR SiPM with active area of 1×1 mm^2 and microcell size of 10×10 μm^2, the noise analysis was performed carefully. The scatter plot of the dark pulse amplitude and time distribution was shown in Fig.3 (a). Each point in the plot represents an event as a function of time interval from the preceding event. The primary events are subject to Poisson distribution theory, being random and independent. Different noise components can be clearly distinguished with the scatter plot [13]. The single cell fired is called 1 p.e. (photoelectron) and the measured amplitude of 1 p.e. pulse was approximately 120 mV. The dots with amplitude around 1 p.e. and located between 30 ns and 10 μs were recognized as primary dark events. Direct crosstalk events were those dots with amplitude of 2 p.e. and 3 p.e. The dots with amplitude lower than 1 p.e. and located approximately between 1 ns and 20 ns correspond to delayed-correlated noise, including afterpulsing and delayed crosstalk. Besides, by analyzing the scatter plot to fit the recovery curve, the recovery time constant for single microcell of EQR SiPM could be easily determined about 2.2 ns that result was verified through the double light pulse measurement [12].

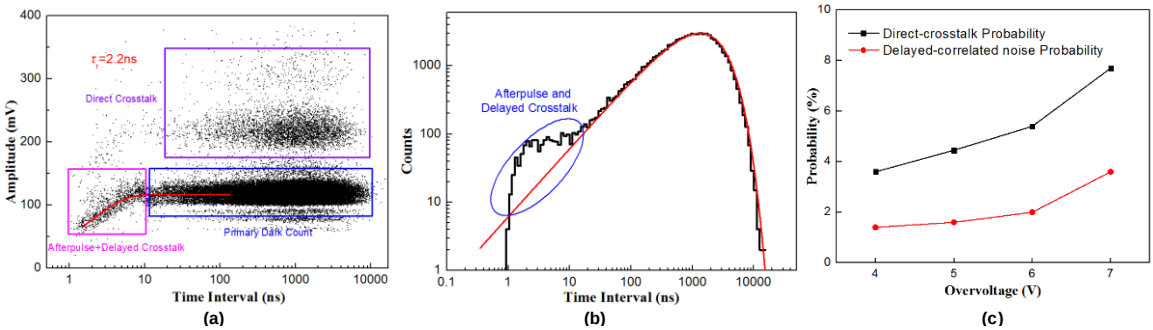

Fig.3. (a) Scatter plot of the dark pulse amplitude versus its time interval from the preceding event at 7 V overvoltage, where draw the fitting recovery curve for single microcell thus obtain τ_r ~ 2.2 ns. (b) Histogram of the time delay array, i.e. projection of the scatter plot on the x axis at 7 V overvoltage. (c) The probability of direct crosstalk (black) and delayed-correlated noise (red) versus overvoltage.

The scatter plot was projected along the time interval axis to obtain the histogram of a time interval statistical distribution shown in Fig.3 (b) [14]. Consequently, the primary dark count rate ~ 700 kHz, the probability of direct crosstalk ~ 7.7% and the probability of delayed-correlated noise ~ 3.6% were obtained at 7 V overvoltage.

We investigated the probability of direct crosstalk and delayed-correlated noise for the EQR SiPM operating in different bias. As shown in Fig.3 (c), the overvoltage reduc-

Proceedings of the 5th International Workshop on New Photon-Detectors (PD18)
Downloaded from journals.jps.jp by Deutsches Elek Synchrotron on 12/12/19

ing, the probability of noise components decreasing. In order to correctly eliminate the influence of delayed-correlated noise on PDE, it is essential to evaluate the noise level for SiPM correctly.

3.2 Single Photon Spectrum and Gain

Fig.4 presents the pulse area distribution of EQR SiPM with active area of 1×1 mm^2 and microcell size of 10×10 μm^2 at 7 V overvoltage, which demonstrates good single photon resolution, and at least 15 p.e. pulse can be distinguished obviously. Through analyzing the pulse area distribution, its gain was measured approximately 2.3×10^5 at 7 V overvoltage. The inset indicates the gain as a monotonous function of the overvoltage.

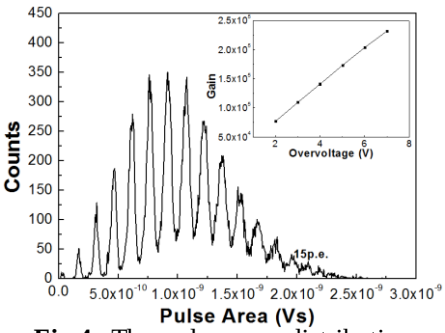

Fig.4. The pulse area distribution at 7 V overvoltage, and the insert shows the gain of SiPM.

3.3 Photon Detection Efficient (PDE)

Comparative study on the PDE characterization with traditional photon counting method, modified photon counting method by noise component analysis and Poisson distribution method were accomplished. Fig.5 show the PDE of EQR SiPM with active area of 1×1 mm^2 and microcell size of 10×10 μm^2 at different wavelength of incident light as 420 nm, 470 nm and 530 nm respectively. Using stochastic photon counting method, the peak PDE reaches 38.6% @ 420 nm under 7 V overvoltage and it is modified to 36.2% @ 420 nm by subtracting the contribution of delayed-correlated noise from the photon counts. However, if the device has too high dark count, it is difficult to effectively achieve noise component analysis because of events accumulated heavily in time distribution [14]. With Poisson method, the PDE of device at 420 nm is about 34%. In conclusion, the result with Poisson method is comparably precise, especially for the SiPM with high dark count rate, because the correlated noise affecting the PDE can be effectively eliminated, and no need for noise analysis.

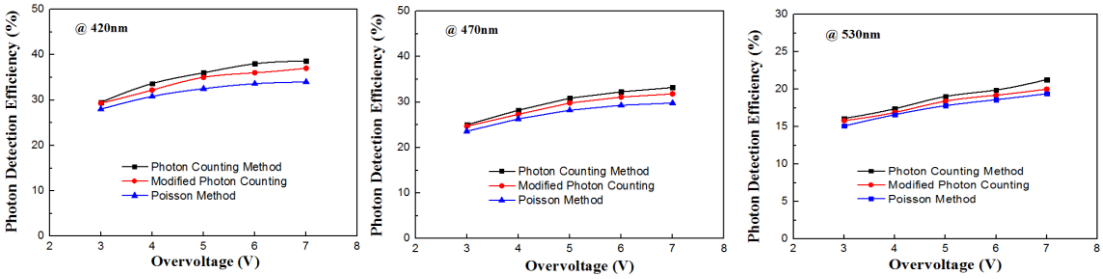

Fig.5. The PDE measured with three methods at wavelength of (a) 420 nm, (b) 470 nm, and (c) 530 nm.

The PDE is attribute to the fact that the EQR SiPM having P-on-N diode configuration is electron-triggered device and that electrons have a higher change of triggering avalanche breakdown. In applications such as Positron Emission Tomography (PET), which require a high sensitivity at blue and violet wavelength band due to presence of the emission spectrum of common PET scintillator (Lutetiμm Orthosilicate (LSO) or Lutetiμm-Yttriμm Orthosilicate (LYSO)) peak in this part of the spectrum [15], these EQR SiPMs are preferable.

3.4 Single-Photon Time Resolution (SPTR)

Time resolution is one of the important characteristic parameters of SiPM that greatly affects the application of SiPM in high energy physics research and time-correlated photon counting technique. The time resolution is determined by the number of photons and SPTR together.

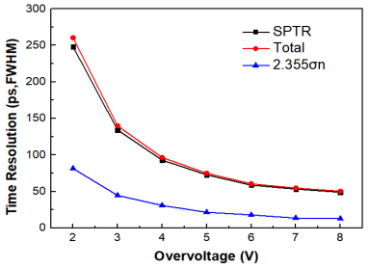

Fig.6. Time resolution measurement.

Proceedings of the 5th International Workshop on New Photon-Detectors (PD18)
Downloaded from journals.jps.jp by Deutsches Elek Synchrotron on 12/12/19

According to the literature [16, 17], the SPTR of 1×1 mm^2 SiPM with microcell size of 50×50 μm^2 was 75-80 ps. As shown in Fig.6, employing a picosecond laser (Nd: YVO_4 pulsed laser, Beijing GK Laser Technology) with frequency of 100 kHz @ 532 nm as the light source, the SPTR of EQR SiPM with active area of 1×1 mm^2 and microcell size of 10×10 μm^2 reaches 53 ps at 7 V overvoltage, which has achieved the international advanced level of SiPM with the same size. The details of measurement and principle are referenced [11].

3.5 Dynamic Range

The dynamic range is proportional to microcell number and also limited. The dynamic range is limited to nonlinear when the amount of incident photons is larger than the number of microcells in the device. The EQR SiPM structure provides benefit to alleviate the contradiction between PDE and dynamic range. As shown in Fig.7, for an EQR SiPM with active area of 1×1 mm^2 and microcell size of 10×10 μm^2, the dynamic range was characterized very close to 10000, which is almost equivalent to total microcell number (~10000). In Fig.7, the experimental dynamic range for high-density EQR SiPM with active area of 3×3 mm^2 and microcell size of 10×10 μm^2 was also presented, which features rather large dynamic range (~90000) while retaining high peak PDE (~32% @ 420 nm) under overvoltage of 5 V at room temperature. The excellent dynamic range performance makes NDL EQR SiPM preferable to those applications requiring a wide range of light intensity detection and high detection efficiency simultaneously.

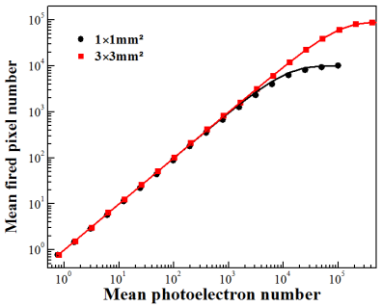

Fig.7. The dynamic range of EQR SiPM with the same microcell size of 10×10 μm^2 and different active area of 1×1 mm^2 (black) and 3×3 mm^2 (red).

3.6 Other Features

NDL has developed new type of EQR SiPM with active area of 1×1 mm^2 and microcell size of 12.5×12.5 μm^2 that has high density as 8000/mm^2. Its DCR is about 750 kHz under 5 V overvoltage, and it can distinguish at least 15 p.e obviously. Comparing with other EQR SiPM, the gain of new SiPM (microcell size of 12.5×12.5 μm^2) is approximately 4.5×10^5 at 5 V overvoltage, which is about twice that of SiPM (microcell size of 10×10 μm^2). This EQR SiPM has high peak PDE of 33.6% @ 420 nm under overvoltage of 5 V shown in Fig.8. Although the PDE of EQR SiPM with larger microcell size and higher fill factor doesn't increase due to its anti-reflection film not being optimized at peak wavelength of 420nm, it performs better for the near red light detection.

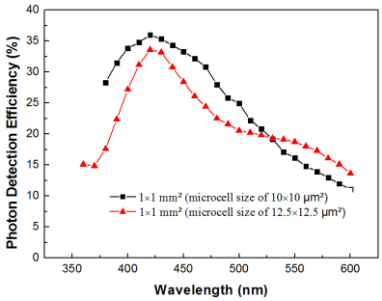

Fig.8. The PDE spectra of EQR SiPM with the same active area of 1×1 mm^2 and different microcell size of 10×10 μm^2 (black) and 12.5×12.5 μm^2 (red).

4. Conclusion

In this report, EQR SiPM with active area of 1×1 mm^2 and microcell size of 10×10 μm^2 demonstrated a peak PDE ~34% at 420 nm while featuring large dynamic range ~10000, the probability of direct crosstalk ~ 7.7% and the probability of delayed-correlated noise ~ 3.6%, the gain ~2.3×10^5, the SPTR ~53 ps (FWHM) and the recovery time ~ 2.2 ns under 7 V overvoltage. It is great benefit to achieve high microcell density while retaining high fill factor, thus it may find applications in a calorimeter of high energy physics where large dynamic range and high PDE are needed simultaneously.

Proceedings of the 5th International Workshop on New Photon-Detectors (PD18)
Downloaded from journals.jps.jp by Deutsches Elek Synchrotron on 12/12/19

Acknowledgment

This work was supported in part by National Natural Science Foundation of China under Grant 11875089 and 61534005.

References

[1]. V.D.Kovaltchouk, G.J.Lolos, Z.Papandreou and K.Wolbaum: Nuclear Inst. and Methods in Physics Research. **A538**, 408-415 (2005).
[2]. https://www.onsemi.cn/pub/Collateral/MICROC-SERIES-D.PDF.
[3]. http://www.hamamatsu.com.cn/UserFiles/DownFile/Product/s12571-010_etc_kapd1044e.pdf.
[4]. C. Li, Z. Chen, Y. Li, B. Li, K. Wang, K. Liang, R. Yang, and D. Han: 2013 NSS/MIC. Seoul, 2013; C. Li, et al: Nuclear Science Symposium & Medical Imaging Conference, (2014).
[5]. A. N. Otte, J. Hose, R. Mirzoyan, A. Romaszkiewicz, M. Teshima, and A. Thea: Nuclear Inst. and Methods in Physics Research. **A 567**, 360-363 (2006).
[6]. Eckert, P., Schultz-Coulon, H. C., Shen, W., Stamen, R., and Tadday: Nuclear Instruments and Methods in Physics Research Section A: Accelerators, Spectrometers, Detectors and Associated Equipment. **A620**, 217-226(2010).
[7]. S. K. Yang, H. Y. Lee, J. A. Jeon, and S. W. Kim: 2013 NSS/MIC. Seoul, 2013; S. K. Yang, et al: Nuclear Science Symposium & Medical Imaging Conference, (2013).
[8]. Z. Guoqing, L. Lina, and L. Hanchen: Optik-International Journal for Light and Electron Optics. **127**, 2936-2938 (2016).
[9]. Dong-Joo Shin, Seongchong Park, Ki-Lyong Jeong, Seung-Nam Park and Dong-Hoon Lee: Metrologia. **51**, 25-32 (2013).
[10]. V. Puill, C. Bazin, D. Breton, L. Burmistrov, V. Chaumat, N. Dinu, J. Maalmi, J. F. Vagnucci, and A. Stocchi: Nuclear Inst. and Methods in Physics Research. **A 695**, 354-358 (2012).
[11]. B. Li, S. Wang, C. Li, T. Zhao, Q. Miao, R. Wang, J. Jia, K. Liang, R. Yang, and D. Han: IEEE Transactions on Electron Devices. **64**, 2239-2243 (2017).
[12]. J. Jiang, J. Jia, T. Zhao, K. Liang, R. Yang, D. Han, Y. Ru, J. Jiali, Z. Tianqi, L. Kun, H. Dejun, and J. Jianquan: Instruments. **1**, 5 (2017).
[13]. C. Piemonte, A. Ferri, A. Gola, A. Picciotto, T. Pro, N. Serra, A. Tarolli, and N. Zorzi: 2012 IEEE. NSS/MIC. California, 2012; C. Piemonte, et al: Nuclear Science Symposium and Medical Imaging Conference, (2012).
[14]. G. Zappalà, F. Acerbi, A. Ferri, A. Gola, G. Paternoster, N. Zorzi, and C. Piemonte: Journal of Instrumentation. **11**, P08014-P08014 (2016).
[15]. S. I. Kwon, A. Gola, A. Ferri, C. Piemonte, and S. R. Cherry: Physics in medicine and biology. 61, L38-L47(2016).
[16]. F. Acerbi, A. Ferri, A. Gola, M. Cazzanelli, L. Pavesi, N. Zorzi, and C. Piemonte: IEEE Transactions on Nuclear Science. **61**, 2678-2686 (2014).
[17]. S. Gundacker, E. Auffray, N. Di Vara, B. Frisch, H. Hillemanns, P. Jarron, B. Lang, T. Meyer, S. Mosquera-Vazquez, E. Vauthey, and P. Lecoq: Nuclear Inst. and Methods in Physics Research. **A718**, 569-572(2013).